30. Bunkin A F et al. *J. Raman Spectrosc.* **37** 693 (2006)
31. Murata K et al. *Nature* **407** 599 (2000)
32. Strel'nitskiĭ V S *Usp. Fiz. Nauk* **113** 463 (1974) [*Sov. Phys. Usp.* **17** 507 (1975)]

PACS numbers: **28.70.+y**, **62.50.+p**, 97.80.Jp
DOI: 10.1070/PU2006v049n08ABEH006080

Nuclear explosions as a probing tool for high-intensity processes and extreme states of matter: some applications of results

V A Simonenko

1. Introduction

Nuclear explosions, along with releasing massive amounts of energy, involve high initial density and intense fluxes of neutron, gamma, X-ray, and electromagnetic radiation, as well as intense radiation, fluid dynamic, electromagnetic, and seismic processes — all this providing a way to study phenomena previously beyond our reach. One example is the self-similarity property of the shock wave flow [1–3] — an important feature of the evolution of high-power explosions in gases, which was already discovered when the first air nuclear explosions were being prepared and carried out and which was later observed and used in laboratory experiments (for example, in the energy diagnostics of high-intensity laser pulses [4]) and in interpreting explosion phenomena in astrophysics.

For explosions of a sufficiently high intensity, assuming a power-law temperature dependence of the heat conductivity, the self-similarity property is also found at an earlier, thermal stage of energy transfer [5, 6]. Such processes occur when radiation and matter have already thermalized but gas-dynamic energy transfer is still negligibly small. The modes of behavior at this stage also carry information about the nonlinear heat conduction properties of the matter involved. Preceding the thermal stage is that of the nonequilibrium propagation of radiation (which was analyzed in [7] for air explosions). The explosion evolution in the air involves a number of gasdynamic, thermal, and optical processes (see monograph [6] for a review), many of which were invoked to justify and apply the methods with which the energy of air explosions was measured.

In Russia, the transition to underground explosions in 1964 posed new problems but also improved opportunities for physical research in the field. Although they share some similar stages with their air counterparts, underground explosions are different in both scale and the underlying physics.

During the period of air tests, only one on-site experiment — the physics experiment of 1957 — was successfully carried out using high-intensity processes for research purposes [8]. With underground explosions, a similar research was begun in our institute in the first on-site experiments and continued until the last test in 1989. The present author has been privileged to have participated in setting up, performing, and interpreting most of these experiments.

This research stimulated efforts to develop theoretical models and mathematical software tools for describing extreme states of matter and high-intensity pulsed processes — work that was paralleled by special-purpose on-site experiments designed to test models and their mathematical realization and to accumulate experimental data. In this way, a science technology including theoretical work, mathematical simulation, and associated experimentation tools and facilities was developed and subsequently further improved, adapted, and applied to new classes of phenomena, such as the interaction of high-power laser beams with matter, the acoustic collapse of microbubbles, high-intensity magnetohydrodynamic processes, and explosion phenomena in astrophysics.

In this talk, the use of explosions as a tool for exploring high-intensity processes and probing the properties of the media involved are briefly described, together with advances in developing theoretical models, and two examples are given to show how other fields can profit from the science technology developed. The first example presents some results on how the threat of small bodies from space (asteroids or comets) hitting Earth can be prevented by using explosions to change their trajectories or to disperse them. The second example discusses a mechanism that governs the propagation of a burning wave on the surface of an accreting neutron star and explains the front modulation of first-type X-ray bursts in low-mass binary systems.

2. General characteristics of explosions and the methodology for their study

The most important features of nuclear explosions are that they are highly localized (typically within dozens of centimeters to several meters) and release huge amounts of energy at a very fast rate (time scale ranging from a few nanoseconds to fractions of a millisecond), with the mass of energy-releasing regions ranging from a few to hundreds of kilograms. The amount of energy released in a nuclear reaction can be larger than ~ 1 MeV per nucleon. Although the energy density averaged over the masses of the energy-releasing regions is lower than that, the matter can reach the temperature 10 keV or more as the energy of the reaction products is transferred to the surrounding atoms. The total explosion energy E_0 varies widely, from fractions of a kiloton to several megatons TNT equivalent ($1\ \text{kt} = 4.18 \times 10^{12}$ J). Because of the high initial temperature, the transfer of the released energy into the surrounding medium first occurs due to radiation. In parallel with this, nonequilibrium neutron and gamma-ray transfer processes operate, which can hinder but can also facilitate doing experiments of high informative value. We note that despite the high energy release density, the energy-releasing regions and the explosive device and its operation supporting system have finite sizes, often comparable to the linear scale of the processes under study (or in use) and must therefore be taken into account in describing the phenomenon.

Underground explosions were carried out in horizontal galleries and vertical holes (see, e.g., Ref. [9]), the burial depth of the charge varying from hundreds of meters to several kilometers, and a specially developed technology ensured the radiation and seismic safety of the experiment. The measurement program was varied on an experiment-to-experiment basis. A special concern was that the conditions at the location of the charge be optimized for conducting the study. While the horizontal scenario is more convenient in this respect, it involves constructing underground workings, drilling holes for instruments, mounting detectors, and

deploying measurement systems and communication channels, which increases the expense. With hole experiments, measurement opportunities were comparatively more limited. In this case, only a limited volume of main holes or, occasionally, of narrow instrument ones was available for mounting the equipment. Experimental setups were assembled on the ground before being lowered to the detonation position together with the explosive device.

In terms of methodology, the following major components can be identified in the study of underground explosions. For the major processes involved, new physical models were developed or already existing ones were used. Often, a complex problem was broken into stages. Based on such models, systems of equations were determined to describe both individual processes and the phenomenon as a whole, and possible initial and boundary conditions were chosen, thus providing standard input data for developing numerical solution algorithms and the corresponding software (with a view to using high computational power). A key aspect of the program was the accumulation of theoretical and experimental data and of software tools for their processing, systematization, and use. Paralleling this were improvements in the relevant physical and mathematical models and programs describing the major processes observed in the tests.

Simultaneously, benchmark experiments were conducted on-site to test the models used, to gather more data, and, ultimately, to justify and further develop the research technology, with the experimental design usually chosen to create as favorable conditions as possible for carrying out specific experimental programs. In many cases, in the preparation of a benchmark experiment, additional experimental research — either in laboratory or as a spinoff of other on-site explosions — was conducted. For all experiments, sufficient computational and theoretical support was provided. Often, benchmark experiments themselves served as preparatory stages for the next generation of experiments.

3. Radiation stage of an explosion

As noted in Section 2, at the early stage of a nuclear explosion, the high-rate high-density energy release from it results in energy transfer by hard (X-ray) electromagnetic radiation even in a dense condensed medium. In this process, the following successive phases are distinguished. The first phase is that of spectral transfer. Next, radiation and matter come to equilibrium with one another and radiative heat conduction dominates. In this phase, the front of the heat wave is bordered by a small region in which, even though spectral transfer still exists, it has no effect on the dynamics of the process. For regions close to the center, there exists a time interval during which radiation energy dominates over that of matter.

For sufficiently high values of the explosion energy, the phase of nonlinear radiative heat transfer may be the longest-lasting one in the list, and it is therefore worthwhile discussing it in some more detail. For explosions as powerful as this, it can be considered that energy is released instantaneously at a point. A further assumption of a power-law dependence of the heat conductivity on the temperature allows the self-similar solution to be used in making the estimates [5].

Early theoretical calculations of the nonlinear heat conductivity (specifically, for astrophysical purposes) used the Rosseland procedure (see, e.g., Ref. [6]) to obtain the average radiation length. While astrophysical media are typically dominated by Compton scattering and bremsstrahlung processes, the analysis of nuclear explosion processes strongly suggested that bound-bound transitions should be taken into account, an understanding which to a large extent came due to the on-site experiment of 1957 [8]. As a result, sufficiently accurate quantum-statistical models were developed for predicting the Rosseland mean free path [10]. By the time of the first underground explosions, a regular supply of this kind of data was established. The 1983 special-purpose experiment [8] highlighted the need for further work to improve the theoretical models used. Although the Rosseland mean free path depends on the temperature nonmonotonically in general, the power-law assumption is quite suitable for purposes of estimation.

With these aspects in mind, we return to considering the heat wave. As the wave propagates, its intensity decreases and its front slows down, and at certain distances acoustic perturbations, due to the temperature gradient and inhomogeneities present in the core regions, start to catch up with the front, resulting in the shock front formation and a change from the thermal (T) to the gasdynamic (G) mechanism of energy transfer. Based on the self-similar solution of the heat conduction problem and equating the heat wave velocity to the speed of sound to define the regime changeover, the characteristic linear scale $r_{\mathrm{T}\to\mathrm{G}}$ for the changeover is found to be

$$r_{\mathrm{T}\to\mathrm{G}} = b(n,\gamma)\left(\frac{\varkappa_0^2 E_0^{2n-1}}{B^{2(n+1)}\rho_0^{2n+2m+1}}\right)^{1/(6n-1)}.$$

Here, it is assumed that the matter obeys the ideal gas equation of state $P = B\rho T$; the Rosseland mean free path is $l = l_0 T^{n-3}/\rho^m$; the constant in the nonlinear heat conductivity coefficient is $\varkappa_0 = 4l_0 ca/3$; c is the speed of light; and a is the constant in the expression for the thermal radiation energy density, $\varepsilon_{\mathrm{th\,r}} = aT^4$. The dimensionless factor $b(n,\gamma)$ depends on the dimensionless parameters n and γ. For rock materials, the characteristic scale is typically $r_{\mathrm{T}\to\mathrm{G}}\,[\mathrm{cm}] \sim 20\big(E\,[\mathrm{kt}]\big)^{0.315}$. As is shown in what follows, it turns out to be compatible with the characteristic size of the gasdynamic motion region at the explosion (see the table). Therefore, viewed from the gasdynamic standpoint, high-power explosions in dense media cannot be considered pointlike.

We recall that for real media, the radiation mean free path depends on temperature in a much more complicated way. In central regions, the radiation energy density may exceed that of matter, suggesting that numerical simulation is needed to obtain a more rigorous description of these processes. Figure 1 presents model calculation results showing the evolution of the heat conduction stage and its transition to the gasdynamic stage for an instantaneous point-like explosion of 100 kt in quartz-containing rock of the initial density 2.65 cm^{-3}. Panel (a) shows the temperature profile evolution. It is seen that at temperatures $T \sim 3-2.5$ keV, the heat wave changes its profile shapes from originally gentle to steeper, stepwise ones, the result of the effective heat conductivity changing at the transition from the radiation-energy- to matter-energy-dominated states. At temperatures $T \sim 1.5$ keV, the shock wave starts to form, as is clearly seen in panel (b) of Fig. 1, which shows density profiles at different times. It may be considered that the shock wave is completely formed by the time the front arrives at the radius ~ 65 cm. This is less than the estimates obtained from the above formula (see the table) because the wave changes its law

Table

Parameter / Medium	High-phase density ρ_0, g cm^{-3}	Initial density ρ_{00}, g cm^{-3}	Speed of sound c_0, km s^{-1}	Dynamic radius r_d, m kt$^{-1/3}$	Regime changeover radius $r_{T\to G}$, m for $E_0 = 1$ kt
Air		1.3×10^{-3}	0.365	289	4.7
Water	1	1	1.5	12.3	0.34
Rock salt	2.16	2.16	3.9	5.03	
Quartzite	4.21	2.65	9.15	2.28	~ 0.19
Granite	3.64	2.56	6.33	3.06	~ 0.17
Dolomite	2.84	2.84	5.25	3.63	~ 0.18
Aluminum	2.7	2.7	5.20	3.85	~ 0.14
Iron	7.85	7.85	3.80	3.33	~ 0.11

of motion at an earlier stage of the explosion, as was noted above.

In many cases, the finite dimensions of an explosive system, r_{NE}, and the size r_{Ng} of the inhomogeneities introduced during the preparation of the experiment are comparable to or even greater than $r_{T\to G}$, further emphasizing the need for numerical calculations. For research purposes (for example, in shock compressibility or opacity studies), 'flat' or 'cylinder' symmetric arrangements were found to be more convenient to arrange. Such experiments used very different installation configurations from possible simplified one-dimensional schemes, making real processes quite difficult to describe. To check the validity of such processes, additional theoretical models and experimental data were used.

The principal results of the study of the early stage of high-energy explosions were that (1) the conditions to optimally ensure the predicted development of processes at the gasdynamic stage were selected; (2) the best suited experimental settings for measuring nonlinear heat conduction properties and ultrahigh compressibility in the heat wave bordering region were selected; (3) new measuring techniques were developed; and (4) major explosion characteristics were measured.

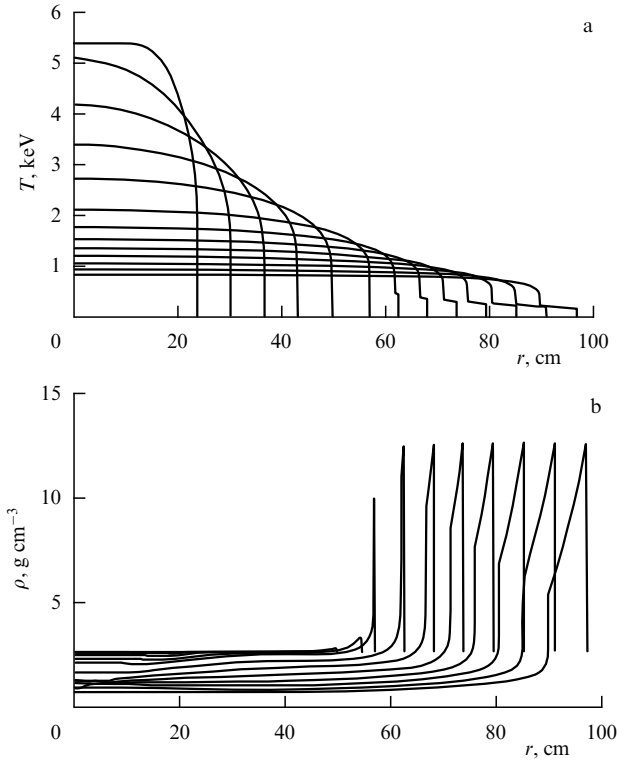

Figure 1. The temperature (a) and density (b) profile evolution for a model explosion with $E_0 = 100$ kt in a quartz-containing medium with $\rho_0 = 2.65$ g cm^{-3}.

4. Gasdynamic stage of an explosion

The change of energy transfer regime primarily shows up in a shock wave starting to form ahead of the heat wave front, whose intensity is subsequently maintained by the energy transfer from the expanding hot matter to cold matter in the region of adiabatic motion. Furthermore, from this point on, the hot matter itself is adiabatically unloaded as it expands. In dense media, the shock-front pressure can reach values of several hundred terapascal (a terapascal is a billion pascals). As the wave propagates, its intensity decreases, and at a sufficiently large distance from the center, the wave front speed D starts approaching a certain effective speed of sound in the medium, c_0, which can be regarded as the limit value for the speed of bulk waves. Closer than this, condensed media behave as compressible matters, for which reason this stage is frequently referred to as gasdynamic, and dense medium compressing explosions, as strong.

For an explosion of energy E_0 in a medium of the initial density ρ_0 and the effective speed of sound c_0, the linear scale of the region of gasdynamic motion is the quantity $r_d = (E_0/\rho_0 c_0^2)^{1/3}$, often referred to as the dynamic explosion radius, and the time scale can be taken to be $\tau_d = r_d/c_0$. The time scale for the heat stage is much shorter than τ_d, and therefore, if matter in the inhomogeneity production region has enhanced heat conduction properties (due to poorly filled cavities, for example), then the explosion energy can be considered to be released instantaneously in a certain effective (energy-release) region whose scale r_E is equal to $r_{T\to G}$ or r_{Ng}, whichever is larger. This makes calculations for the gasdynamic stage easier in some cases. In more complex cases, however, an accurate description of gasdynamic processes requires that the major inhomogeneities created in carrying out experiments should even be taken into account at the early stages of the phenomenon.

For a sufficiency large region of gasdynamic motion to form in the surrounding medium, the scale r_E must be much smaller than r_d. The above arguments apply equally to gaseous and condensed media; however, although the dynamic radius r_d is formally defined in the same way for gases and dense media, there is a fundamental difference between them that influences how the processes involved occur. For condensed media, at not very high temperatures characteristic of the adiabatic stage of the explosion, equations of state (i.e., the dependence of the pressure P and internal energy ε on the density and temperature) can be

written as a sum of cold (c) terms (due to the elastic interaction of atoms) and thermal terms,

$$P = P_c(\rho) + P_T(\rho, T)\,, \qquad \varepsilon = \varepsilon_c(\rho) + \varepsilon_T(\rho, T)\,.$$

Equations of state for gaseous media contain no cold terms, the quantity c_0 is determined only by thermal motions, and the product $\rho_0 c_0^2$ is, up to a constant of the order of unity, the initial thermal pressure. Importantly, the deviation from self-similarity is due to the effect of the initial pressure of the gas ahead of the wave front. In condensed media, the value of c_0 is determined by quantum mechanical interactions, the density of matter is significantly larger than in gases, and the product $\rho_0 c_0^2$ greatly exceeds the initial static pressure. The dynamic explosion radius in dense media can be dozens or even hundreds of times smaller than that in gaseous media (see the table). The initial ahead-of-the-wave-front pressure can still be left out of account, and the deviation of the self-similar solution is determined by the presence of 'nonideal' terms in the equation of state. For explosions in dense media, the condition that the scale r_E is smaller than r_d becomes a more acute problem. Indeed, because this condition cannot be satisfied for some values of the explosion energy, special measures were taken to decrease r_E when preparing experiments to study gasdynamic processes.

Some types of rock, in particular, quartz-containing ones, demonstrate very clear and kinetically very complex polymorphism when shock-loaded. Experimental studies of this phenomenon, including those using on-site experiments, have been ongoing for many years, but it is only in recent years that satisfactory models have been developed. Early work was limited to the effective description of flow in high-density phases, a region where the large values of the parameters ρ_0 and c_0 further reduced the region within which interpretable results could be obtained.

The table in Section 3 presents the initial values and estimated scales of r_d and $r_{T\to G}$ for some typical rocks, for air, and for water. Also included for comparison are similar values for aluminum and iron, although their use as host media is unlikely to be economical.

We consider the abstract problem of an instantaneous point-like explosion in a dense medium. The solution of this problem exhibits a region in a certain neighborhood of the explosion center in which the shock wave flow can to good accuracy be treated as self-similar (with wave front pressures close to the limiting ones) and whose size is $\sim 0.1 r_d$ for typical media. We now restate the problem by considering a point-like explosion in a medium with nonlinear heat conduction as the energy transfer mechanism at large energy densities. The transition of the gasdynamic transfer mechanism then occurs at $r_{T\to G} \sim (0.06-0.09) r_d$ according to the table. In some artificial media, the ratio $r_{T\to G}/r_d$ can be somewhat less than that, but even then it is sufficiently large, thus leaving us with two distinct stages, heat-conduction and gasdynamic. We note that the timescale of the heat conduction stage is very small, and therefore, to a certain approximation, gasdynamic flows produced in strong explosions can be treated by assuming that energy is reloaded instantaneously in a region comparable in size to the radius over which the transfer mechanism changes. We are actually dealing with the problem of an instantaneous non-point-like explosion.

Therefore, developing detailed theoretical models of individual processes to describe the explosion phenomenon as a whole requires a high enough level of software power, accurate information of the thermodynamic and heat conduction properties of materials and media, and vast experimental and theoretical databases.

In the experimental studies of shock-wave flows created in the explosion, not only integral parameters but also local parameters — the ones characterizing its intensity — were used to verify physical models and mathematical codes. The shock wave itself was used to directly study the shock compressibility of various materials, including rocks from the explosion site (see Section 5).

Two other areas of computational, theoretical, and experimental explosion research were related to two classes of two-dimensional gasdynamic flows in dense media. One area was the study of how the shape of the shock wave front evolved in time following its initial distortion by inhomogeneities in central regions bordering the energy release region. It turned out, in particular, that for typical rocks, the 2 : 1, 3 : 1 prolate shape of the front in the $r_{T\to G}$ region becomes less prolate and changes phase with increasing distance, resulting in an oblate shape. However, while the front shape becomes less distorted as the wave moves away, still the distortions do not disappear, even far away at the boundaries of the gasdynamic region. The second area was concerned with shock shape distortions due to the presence of filled channels that were involved in experiments either for technological or research optimization purposes. In some cases, the shock wave had to be made to lag behind in the channel, in others, on the contrary, to take over (for example, in the gamma benchmark technique). In some experiments, accurate measurements of the wave front shape were performed and compared with the results of detailed calculations. These studies, in addition to solving specific problems, were instrumental in the development and improvement of algorithms and codes used to describe two-dimensional gasdynamic flows.

5. Exploring the properties of matter

The transition to underground explosions naturally led to the idea that the high-intensity processes they involve might be used to probe the properties of matter in extreme states unachievable in laboratory — the first candidate process being of course a shock wave propagating in the ambient medium. By that time, experience had already been gathered in studying shock compressibility using shock waves produced by condensed explosives [11], and extending the existing methods to high pressures difficult or impossible to achieve in laboratory experiments was a natural step to take.

The need for such data was driven by the search for wide-range equations of state that were required, in particular, for describing explosions in dense media. In the early 1960s, equations of state were developed based on either data from laboratory experiments (in the region of relatively low pressures, Ref. [11]) or data from the quantum-statistical Thomas – Fermi model (high pressures, Ref. [12]). Later, in describing the electronic component of the system, Russian researchers started using N N Kalitkin's [13] revised quantum-statistical data with regular quantum corrections. To include the ionic contribution, the one-component plasma approximation was typically used, in the form of a relation proposed by V P Kopyshev [14]. A rather big gap remained between experimental and theoretical data, where no data were available. A sufficiently strong shock wave from an underground explosion was quite capable of bridging this gap.

The most convenient way to conduct this kind of research was by employing the method of reflections, in which the shock wave passed successively through a plate of a reference substance and one of the material under study. Compounding the situation, however, was the lack of high-pressure reference data, which often restricted measurements to those of relative compressibility. For conducting underground studies, new experimental arrangements and detection schemes were designed and new types of detectors were developed. We note that because of quite favorable background conditions, many measurements used electric-contact sensors, as did many shock-wave experiments then performed in the country. The first, but nevertheless full-scale, experiment of this type was already conducted at our institute in 1966 [8]. The ability to work with big samples provided the additional possibility of accurately measuring the dynamic susceptibility of porous materials and mixture compositions [15].

Shock-wave studies using a wave in a medium are only feasible if the gasdynamic region is sufficiently large, that is, at high-yield explosions. Such experiments are expensive and relatively rare. Traditionally, they were mostly conducted at the VNII (All-Union Research Institute) of Experimental Physics, first with L V Al'tshuler and then with R F Trunin directing the shock-wave research as described above [16].

Along with just expanding the pressure range of shock-wave studies, long-base measurements proved to be a valuable option and were successfully used in a series of on-site experiments to study the kinetics of polymorphic transformations in quartz [17]. It was shown that the transition of quartz into a high-density phase in on-site experiments causes the shock wave to bifurcate, something that does not have enough time to occur in small laboratory samples. Also, the precision measurements of the shock-wave speed in a number of on-site experiments on quartz revealed that the melting of quartz affects the way in which the wave attenuates with distance. These data, together with the results of precision laboratory experiments, are used even today to better describe the behavior of quartz in dynamic processes [18]. Experiments were also made to study graphite-to-diamond transformations.

To explore shock compressibility at the extremes of high pressure, it was suggested at VNIITF to use flows in the layers bordering the $r_{T\to G}$ region. The level of pressure in such layers is always determined by the transition of the heat wave to the shock wave, and hence, by manipulating the transition temperature, waves of various intensities can be obtained. At the highest temperatures, the shock waves can reach their limit intensities $P \gtrsim 1$ Gbar, whereas by lowering temperature, waves of medium intensity $P \sim 10-100$ Mbar can be obtained at relatively large distances from the energy source. It turned out that, paradoxical as it may seem, doing research in this way is even easier at very high pressures than at high-yield explosions. However, a number of problems had to be solved first. Because this scheme places measuring units at small distances from the charge, protection from the neutron and gamma backgrounds must be provided, and because, further, contact sensors do not operate under such conditions, a special time-interval measuring technique was developed that optically determined the arrival times of the shock wave at the control levels. The technique used specially designed channels to detect light flashes that occur when the wave front arrives at the dense matter – gas interface. Because of the smaller scale of the phenomenon, smaller samples had to be used, increasing measurement accuracy and detection system requirements. Precisely this scheme provided high-precision compressibility data on a number of materials for the region close to applicability limits of quantum-statistical models.

It became clear to us in the 1970s that this pressure range needed to be studied experimentally. Although the models of matter being developed at the time were still rather simplistic, they clearly identified electron shells as a factor that could have an effect on the properties of matter close to this boundary, the size of the effect varying widely — and in some cases being very large — depending on the model used [19]. Therefore, in parallel with developing experimental techniques and preparing the master experiment, theoretical models were revised and improved [20, 21]. Data from this work were used as a reference when deciding on the goals and methodology of an on-site experiment. The 1983 master experiment produced high-precision relative compressibility data, at record pressures of hundreds of megabars, for the Fe–Al, Fe–Pb, and Pb–Fe pairs, with eight data points for each (the first metal in the pair is a reference one). Besides, additional data for these substances, as well as for water and quartz, were obtained in preparatory experiments, which confirmed that shell effects need to be studied more carefully. The choice of iron as a reference was also successful in allowing a sufficiently accurate determination of normal shock adiabats for aluminum at $P = 40-250$ Mbar and for lead at $P = 80-500$ Mbar; the adiabats were found to oscillate with respect to the quantum-statistical dependences [22, 23].

Data on mean free paths in Al and Fe, also obtained in this experiment, suggested that the results from quantum-statistical models needed to be corrected — in particular, by as much as $\sim 20-30\%$ in the temperature range $0.7-1.5$ keV at the density 1 g cm^{-3} [8, 23].

Along with gasdynamic processes, neutron fluxes produced by nuclear explosions were also used in shock-wave studies. An example is the gamma benchmark method, which consists in measuring the speed of a substance (aluminum) behind the shock front at the pressure about 10 Mbar. The method involved introducing pellets with europium into the aluminum block [europium nuclei have an enhanced (n,γ) cross section for neutrons with an energy $\varepsilon_n \lesssim 100$ eV] and it was suggested setting up the experiment such that the arrival of the shock and the neutron deceleration to the required energies be synchronized in the measuring block region. Detection was performed by using plane collimators mounted parallel to the shock-front surface moving in the sample (shock wave motion in the aluminum block was created using a magnesium-filled channel with the property that a wave propagating in the channel took over the wave in the surrounding medium). Data from this method confirmed that using iron as a reference is quite appropriate for the lower-pressure range of the relative shock compressibility measurements of aluminum [24] that were performed to assess the shell effects.

The generation of shock wave motion was yet another application of intense neutron fluxes. For this purpose, a plate of a fissionable material was introduced into experimental assemblages that were placed in such fluxes. Such measurements were made as part of experiments to study the discharge of heated matter and the associated shock wave motion. In particular, American researchers used (and we tested experimentally) a method which employed the Doppler

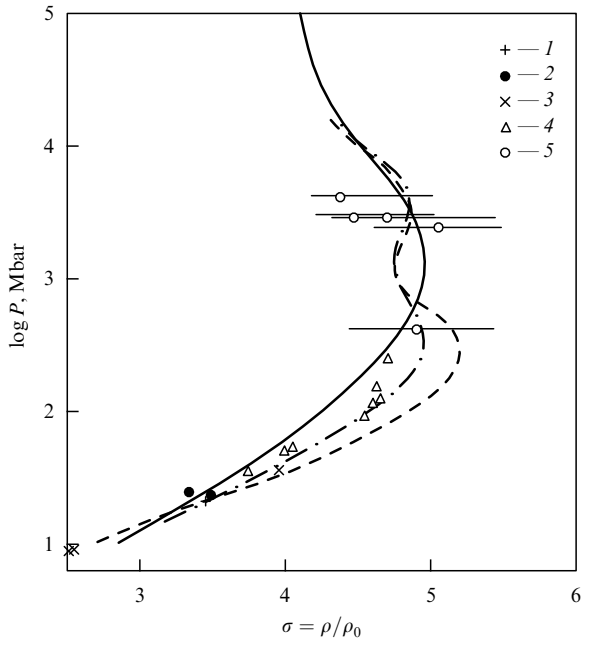

Figure 2. Theoretical and experimental data for the shock compressibility of Al from research using nuclear explosion experiments. Solid line is for the corrected Thomas – Fermi model [13, 14]; dot-dashed line, for the self-consistent field model [20]; and dashed line, for the Hartree – Fock – Slater model [10]. Experimental data: *1*, [16]; *2*, gamma benchmark technique [24]; *3*, [26]; *4*, precision data obtained in the region of oscillations [22]; and *5*, crude data from the quantum-statistical model in its validity range [23].

shift of neutron absorption resonances to measure the mass velocity behind the shock front [25]. Unfortunately, this method proved to be rather inaccurate.

As an example of the use of shock wave processes for the comprehensive study of matter properties, Fig. 2 shows the experimental data on the shock compressibility of Al obtained by our group and by VNIIEF [16] and American [26] researchers. For comparison, data from theoretical models are given. (We note that our results include precision data for the regions where the effect of the first electron shell is important.)

To summarize, nuclear explosion experiments provided the following data:

- the shock compressibility of a number of dense and porous materials and mixture compositions at pressures that are hard, if not impossible, to achieve in laboratory studies;
- the manifestation of electron shell effects in the shock adiabats of Al, Fe, etc.;
- phase-transition dynamics; and
- the Rosseland radiation mean free path in A and Fe.

These data are used even today as a reference in developing theoretical models of matter and constructing phenomenological equations of state.

6. Explosion effects on small space bodies

A clear fact that has emerged from research in different disciplines over the last decades is that ours is an epoch in which the Earth is undergoing encounters with small space bodies like asteroids and comets and their fragments — on a timescale that is longer than, comparable to, and smaller than those of a human life, a civilization, and a geological period, respectively. Such encounters may lead to catastrophic consequences — at the local, regional, or global level, depending on the size of the body — and, in the worst case scenario, may even trigger the destruction of civilization and indeed of humanity as a whole. The event rate of such encounters varies approximately inversely with the square of the size of the body.

We first discuss asteroids in some detail. So far, most of the larger — globally threatening — asteroids and only a fraction of small-size ones have been discovered. Asteroid monitoring programs are being expanded. Several asteroids with nonzero impact probabilities have been discovered. The asteroid expected to threaten Earth first is known as Apophis, discovered in 2004. In 2029, Apophis will fly by at the distance about 30,000 km from Earth, and if unfavorably deflected in its course, may collide with it in 2036. As more observations accumulate, more certain forecasts will come to replace probabilistic estimates.

Given the densely populated and dangerously technologized nature of global geography, even the events such as the Tunguska blast (with the impact energy about 15 Mt) may be extremely disastrous, so all the more Apophis, 350 m and with the predicted impact energy 1.5 Gt. Wherever it hit, there would be a catastrophe of vast proportions at the regional level — with possible devastating consequences globally. It is therefore clear that some technology should be developed to prevent this from happening. Analysis of possible collision prevention technologies has pointed to the nuclear explosive charge as the only state-of-the-art solution possible. In this case, thanks to the high energy densities involved, even a small mass can produce the necessary energy levels — allowing already existing rockets to be used to deliver these systems to the threatening objects and to deploy them on their surface in an optimal way. Clearly, the experience gathered in conducting peaceful explosions could be used to advantage in this case, as could the technology that has been developed for their description.

In the above context, three regimes in which a single nuclear explosion could be conducted for this purpose — standoff, on-surface, and buried [26] — have been explored; major energy transfer mechanisms (radiation, gasdynamic, and neutron flux) have been analyzed for their roles in this scenario; and how the deflecting momentum forms under typical conditions has been examined. It has been found that for bodies made of high-strength materials, the on-surface approach would be most efficient. However, in more complex deflection problems, other scenarios could be used as well (for example, to divert low-strength, porous bodies like the asteroid Itokawa). The efficient deflection of objects of complex shape and composition would require that multiple explosions be employed, in which case the energy of each of them, as well as their arrangement and time separations, should be optimized.

Depending on the warning time (which ranges from years for large, globally threatening bodies to days or months for those capable of inflicting regional or local damage), two orbit-modification approaches are conceivable [27].

The 'soft' approach could be used when warning times measure in years and applies to large- and medium-size bodies with sufficiently high strength properties. The energy of the explosion(s) and its (their) position(s) on the surface are chosen in such a way as to ensure the momentum transfer required for the correction and, importantly, to avoid the destruction of the body. A reliable assessment of the possible effect of the explosion requires a comprehensive study of the properties of the object, thus calling for one or more space

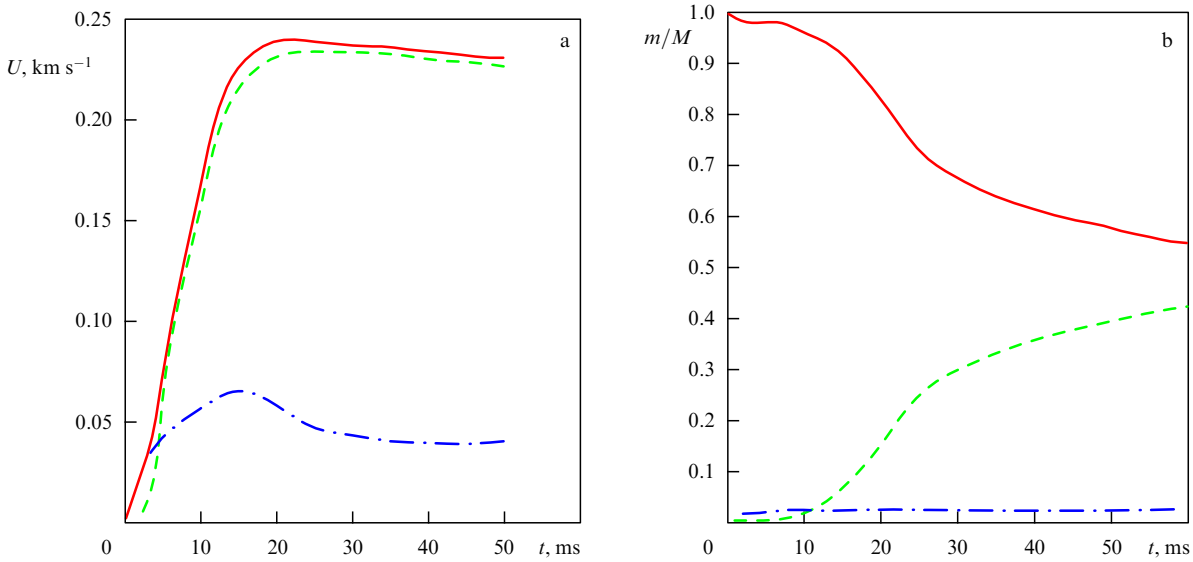

Figure 3. (a) Formation of the momentum of the fragment distribution: solid line, total velocity; dashed and dot-dashed lines, components perpendicular and parallel to the force, respectively; (b) Destruction of the body: solid line, intact mass fraction; dashed line, destructed fraction; dot-dashed line, mass fraction in the jet.

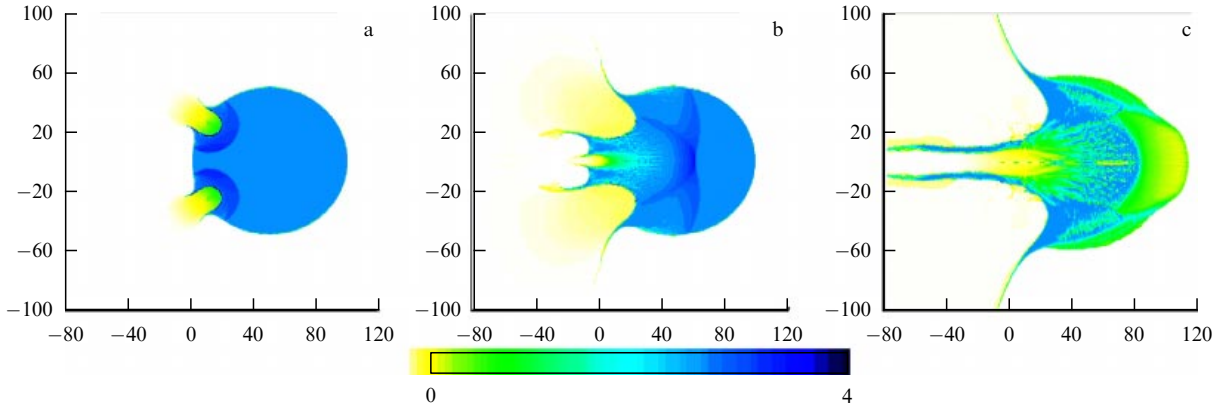

Figure 4. General picture of the formation of the distribution of fragments and the jet in the form of density profiles at times 3, 10, and 40 ms (for the example in Fig. 3). The axes use linear scales in meters; change in density (in g cm^{-3}) is represented by the linear intensity of darkening in accordance with the intensity scale shown.

research missions to be sent to it. The results thus obtained are necessary for choosing the energies, arrangement, and time pattern of the explosions. If an especially soft modification is needed, more than one series of explosions could be conducted.

The most likely and, if it arises, highly urgent scenario in the impact hazard field is one with a warning time on the scale of days or weeks. In this case, the space body would have to be impacted with a very large momentum to be prevented from hitting Earth. The body would then inevitably be dispersed, most of its mass becoming debris — which would fly by at a safe distance from the Earth — and a minor part being ejected as a jet of gas, dust, and small particles. Figure 3 depicts the formation of momentum and the destruction process for a spherical (to simplify the calculation) stony body 100 m in diameter subjected to a 100 kt buried explosion distributed over a circumference of diameter 50 m. Figure 4 depicts the destruction process by showing the density distribution for three moments in time. Although some of this material would interact with the earth's atmosphere and radiation belts and would thereby lead to some adverse effects (like anomalous magnetic phenomena and damage to satellites), this would of course be much less disastrous than what the intact body would inflict. As in the previous case, a synchronized detonation of multiple charges is also worth considering here if a more reliable prediction of what will happen is needed. The optimization criteria to be used in choosing the explosion scheme should be the reliable prevention of the impact and the minimum adverse effect on the radiation belts and the atmosphere.

By using a similar conceptual scheme, long-period comets can also be prevented from striking Earth. Unfortunately, however, the properties of comets are even less known. In particular, there is a danger of the cometary core being disintegrated by the explosion. In addition, comets move in larger orbits that are sometimes parabolic, or nearly so, the knowledge of which is typically far from certain. Furthermore, studying dangerous comets and exerting the necessary effect on them would require planning on an urgent basis of long-term, flexible, in-flight programmable missions (to

include, for example, task switching from research to interception and vice versa).

In summary, the science and technology developed for solving the problems we have outlined are in demand for the future studies of small space bodies, most importantly in the context of preventing them from colliding with Earth.

7. Thermonuclear burning on the surface of a neutron star

Progress in X-ray astronomy in the last three decades has opened up new possibilities for the observation of neutron stars that are in the active phase of their evolution. Among these, bodies known as X-ray bursters, identified as members of binary systems, are of special interest. The accretion of matter from its companion star ensures a sufficiently high background luminosity of the neutron star, of the order of 10^{37} erg s^{-1}, which, however, is not constant in time due to variations in the flux of the accreting matter. This enables one to estimate the matter accumulation rate $\dot{M}$ for the neutron star. A number of objects against this luminosity background show pulse flux increases by a factor in the dozens, with the leading edge around 1 s or less, the trailing edge from several to dozens of seconds, and the burst separation ranging from hours to days. The ratio of the burst energy to the overall energy of the calm stage suggests that the bursts are thermonuclear in origin. It turns out that the technology developed for describing high-intensity explosions can be very useful for describing thermonuclear neutron star bursts [28].

The matter that comes from the companion star forms a surface layer, often referred to as the atmosphere. As this matter moves deeper into the atmosphere, it changes in composition due to thermonuclear and picnonuclear reactions, and becomes stratified. In particular, some neutron stars have a layer of mainly helium formed $10^7 - 10^8$ g cm^{-2} deep in their atmosphere, in which appropriate temperature conditions for the fusion of three helium atoms arise at a certain time. If conditions in this layer are relatively uniform along the entire surface, then the entire star is very soon involved in the process of thermonuclear burning (for the burning to be synchronized, even a weak adiabatic gravitational wave propagating at about 10^8 cm s^{-1} suffices). This type of regime occurs when the matter is relatively slow to accrete, and the development of this phenomenon is well modeled by one-dimensional calculations. According to our studies [29], a fundamentally important fact here is that the primary transport mechanism for the released energy is convective turbulence, which is faster than radiative heat conduction in delivering energy to the upper atmosphere and which enables helium to burn-out uniformly in the atmosphere, as shown in Fig. 5.

If the accretion rate is sufficiently high, the burning process is triggered locally (some regions of the layer being still unprepared for self-ignition). However, conditions may exist under which the burning propagates along the star surface (although the burning wave propagates much more slowly than the adiabatic gravitational wave). A feature of such bursts is distinct leading-edge oscillations. The high rotational frequency of the neutron star (up to and beyond 300 Hz) results in the burning region periodically being out of the field of view (mostly only in part) — hence the intensity modulations. After all or nearly all the surface has started burning, a similarly nonuniform cooling process follows, resulting in the falling part of the pulse being modulated.

Those still cold portions of the helium layer that border the burning region start to burn due to the flying out burning

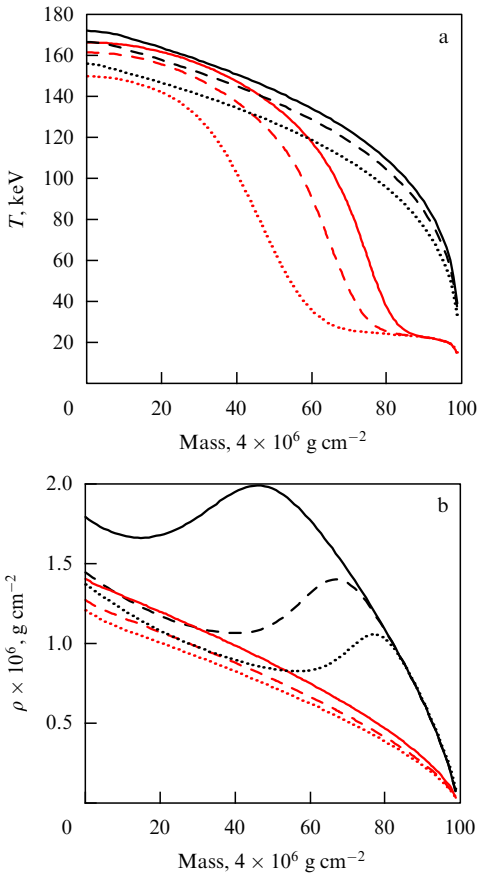

Figure 5. Simultaneous bursts across the surface of a neutron star atmosphere with and without taking the turbulence mixing into account (smoother curves and those with a distinct compression wave profile, respectively) for three time instants: 0.066 ms (solid lines), 0. 085 ms (dashed lines), and 0.10 ms (dotted lines). Temperature (a) and density (b) profiles as functions of mass expressed in percent of the total mass of the atmosphere (which is 4×10^6 g cm^{-2}).

products inflowing to the upper atmosphere. This inflow produces some additional compression and increases the temperature at the bottom of the helium layer bordering the burning region. This provides conditions for ignition, and this configuration moves over the surface of the neutron star. In this way, a self-maintaining thermonuclear burning regime forms due to the gravitational compression of matter by burning products flowing from above. This mechanism of burning in the helium layer was investigated using the two-dimensional codes TIGR (finite-difference Euler – Lagrange method) and MPM (modified particle method) [29]. Figure 6 shows modeling results for this process. The estimated burning wave speed, $5 \times 10^6 - 10^7$ cm s^{-1}, is in good agreement with the observational data.

One further point to mention is that a localized thermonuclear burst excites an adiabatic gravitational wave propagating along the atmosphere. The focusing of this wave in the antipodal area involves an additional inflow of matter [30], with the possible result that under favorable conditions, thermonuclear ignition synchronized with the primary one is triggered in the antipode, with thermonuclear burning therefore propagating over the star surface from two regions. This type of regime presumably occurs for bursters with the modulation frequency about 600 Hz.

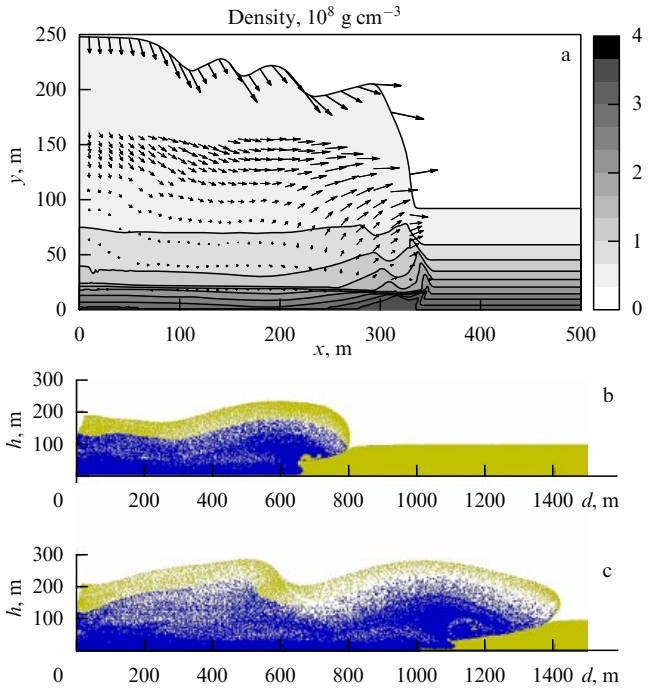

Figure 6. Formation of a thermonuclear burning wave in the gravitational self-shrinking regime. Panel (a) (obtained using the TIGR code for the atmospheric thickness 1.8×10^7 g cm^{-2}) shows density profiles in units of 10^8 g cm^{-3} (linear intensity scale of densities is shown on the right) and the velocity vector field (arrows) reflecting the inflow of matter and increase in the density of the lower layer. Panel (b) is obtained using the MPM code for the atmospheric thickness 1.8×10^8 g cm^{-2}. Light points correspond to the initial substance, helium; burning products are shown dark. The inflow of burning products along the upper boundary of the atmosphere is readily seen. h is the height of the atmosphere and d is the traveled path.

This then is another example of where the technology developed for describing explosion phenomena can be usefully applied.

8. Conclusion

The study and use of high-intensity processes involved in nuclear explosions has provided valuable insights both into how these processes evolve and into the relevant properties of the media involved.

For the first time in terrestrial experiments, high-temperature thermal processes due to nonlinear radiative heat conduction were explored and used. Under the conditions of energy transfer changing from the heat to gasdynamic regime, heat conduction data for materials in high-temperature dense plasma environment were obtained. These data stimulated further work on theoretical models, which, in this context, are the primary source of information on the heat conduction properties of materials in this field.

The shock wave flow that results from a regime changeover is the most intense adiabatic flow experimentally achievable for such high-density media. It was shown that strong explosions in media of currently accessible densities, in fact, show no region of self-similar motion — first, because the region where energy is transferred by heat is relatively large (making the effective energy release 'non-point-like'); and, second, because the region of gasdynamic motion is relatively small. The subsequent evolution of the shock is strongly affected by such factors as the quantum mechanical nature of particle interactions in dense matter, phase transition phenomena (melting and, possibly, polymorphic transitions), and strength properties. The evolution of polymorphic transition is often complicated by kinetic effects.

Shock waves from nuclear explosions were directly used to extend shock compressibility measurements of dense materials to the high-pressure range, as well as for compressing highly porous and mixture samples. Through the use of such explosions, unique data on the shock compressibility of a number of materials and rocks at pressures beyond the laboratory scale were obtained. Moreover, precision shock compressibility measurements at the applicability limit of quantum-statistical models were made, which not only confirmed that electron shell effects influence the course of a normal shock adiabat but also provided an accurate description of the shock adiabat behavior in the region of the first oscillation for Al and Fe. Detailed studies of shock wave attenuation in massive quartz revealed the influence of melting processes and enabled the observation of the two-wave mode in the region of dynamic transformation of α-quartz to the high-density phase — a regime that has not been observed in laboratory experiments. These data are being used even now in constructing more accurate theoretical models of the behavior of dense matter both at high pressures and temperatures and in the region where phase transitions show up and strength properties become relevant.

Importantly, there was a strong preparatory component to research on nuclear explosions, including a complex of laboratory experiments (on low-pressure shock compressibilities and on modeling some relevant processes) and work on the mathematical simulation of both individual processes and the explosion as a whole based on the already existing physical models, software packages, and adequate computational means. In turn, the results of on-site experiments were used to improve and develop these tools.

Thus, on the one hand, the experimental results stimulated the development and improvement of physical and mathematical models and of computer programs, whereas on the other hand, the results of mathematical simulation allowed more sophisticated experiments, extended the scope and range of research, and provided more accurate experimental data. In fact, research into processes involved in nuclear explosions resulted in a scientific technology for probing the physics of high energy densities — a technology in which physical models and simulation method development and on-site and laboratory experimentation are naturally integrated. As a result, a vast research potential was built up, so vast, indeed, that even today this technology is being successfully developed, taking advantage of the power of modern experimental techniques, using advanced simulation software and enhanced computational capabilities, and finding ever more applications. To illustrate these points, two examples are given in the text.

The first example is concerned with the study of nuclear explosion effects on Earth-threatening space objects like asteroids and comets and their fragments. The effects of standoff, on-surface, and buried explosions have been examined, and the most effective ways in which the energy and momentum of an explosion can be transferred to a threatening body to prevent its collision with Earth (specifically, two extreme scenarios — a 'soft' orbit modification and a high-speed dispersion of the body) have been considered. At the current level of technology, nuclear explosions are the only (and also quite feasible) way to prevent dangerous collisions.

The other example is pulsed thermonuclear burning on the surface of a neutron star in a low-mass binary system. For this scenario, the convective-turbulence-mediated transfer of the released energy is shown to be fundamentally important. If the accretion rate is sufficiently low, this mechanism accelerates the delivery of energy to the surface and leads to the uniform burnout of the thermonuclear fuel. For a high accretion rate, the burnout process starts in the region that is most prepared for this and propagates along the surface in the form of a wave in the gravitational self-compression regime.

The list of examples could be extended to include both low-energy (but high-power) explosive processes (found, for example, in superintense laser pulses) and still higher energy ranges (e.g., supernova and hypernova explosions).

References

1. Sedov L I *Dokl. Akad. Nauk SSSR* **52** 17 (1946); *Prikl. Mat. Mekh.* **10** 241 (1946); *Metody Podobiya i Razmernosti v Mekhanike* (Similarity Methods and Dimensionalities in Mechanics) (Moscow: Nauka, 1987) [Translated into English (Moscow: Mir Publ., 1982)]
2. Stanyukovich K P *Neustanovivshiesya Dvizheniya Sploshnoi Sredy* (Unsteady Motion of Continuous Media) (Moscow: GITTL, 1955) [Translated into English (New York: Pergamon Press, 1960)]
3. Taylor G *Proc. R. Soc. London Ser. A* **201** 175 (1950)
4. Basov N G, Lebo I G, Rozanov V B *Fizika Lazernogo Termoyadernogo Sinteza* (Physics of Laser Fusion) (Moscow: Znanie, 1988)
5. Zel'dovich Ya B, Kompaneets A S "K teorii rasprostraneniya tepla pri teploprovodnosti, zavisyashchei ot temperatury" ("On the theory of heat transfer with a temperature-dependent heat conductivity"), in *Sbornik, Posvyashchennyi 70-letiyu Akademika A.F. Ioffe* (Collection in Honor of the 70th Birthday of Academician A.F. Ioffe) (Moscow: Izd. AN SSSR, 1950)
6. Zel'dovich Yu B, Raizer Yu P *Fizika Udarnykh Voln i Vysokotemperaturnykh Gidrodinamicheskikh Yavlenii* (Physics of Shock Waves and High-Temperature Hydrodynamic Phenomena) (Moscow: Nauka, 1966) p. 519 [Translated into English: *Elements of Gasdynamics and the Classical Theory of Shock Waves* (New York: Academic Press, 1968)]
7. Kompaneets A S, Lantsburg E Ya *Zh. Eksp. Teor. Fiz.* **43** 234 (1962) [*Sov. Phys. JETP* **16** 167 (1963)]
8. Avrorin E N, Simonenko V A, Shibarshov L I *Usp. Fiz. Nauk* **176** 449 (2006) [*Phys. Usp.* **49** 432 (2006)]
9. Mikhailov V N et al. (Eds) *Yadernye Ispytaniya SSSR* (Nuclear Weapons Tests of the USSR) Vol. 1, 2 (Sarov: Izd. PFYaTs — VNIIEF, 1997)
10. Nikiforov A F, Novikov V G, Uvarov V B *Kvantovo-statisticheskie Modeli Vysokotemperaturnoi Plazmy: Metody Rascheta Rosselandovykh Probegov i Uravnenii Sostoyaniya* (Quantum Statistical Models of High Temperature Plasma and Methods for Calculating Rosseland Mean Free Paths and Equations of State) (Moscow: Fizmatlit, 2000) [Translated into English: *Quantum-statistical Models of Hot Dense Matter: Methods for Computation Opacity and Equation of State* (Basel: Birkhäuser Verlag, 2005)]
11. Al'tshuler L V *Usp. Fiz. Nauk* **85** 197 (1965) [*Sov. Phys. Usp.* **8** 52 (1965)]; Al'tshuler L V et al. *Usp. Fiz. Nauk* **166** 575 (1996) [*Phys. Usp.* **39** 539 (1996)]
12. Latter R *Phys. Rev.* **99** 1854 (1955)
13. Kalitkin N N, Kuz'mina L V "Tablitsy termodinamicheskikh funktsii veshchestv pri vysokikh kontsentratsiyakh energii" ("Tables of thermodynamic functions of materials at high energy concentrations), Preprint No. 35 (Moscow: IPM AN SSSR, 1975)
14. Kopyshev V P "O termodinamike yader odnokomponentnogo veshchestva" ("On the thermodynamics of nuclei in a one-component material"), in *Chislennye Metody Mekhaniki Sploshnoi Sredy* (Numerical Methods in Mechanics of Continua) Vol. 8, Issue 6 (Novosibirsk: VTs ITPM SO AN SSSR, 1977) p. 54
15. Vildanov V G et al., in *Shock Compression of Condensed Matter — 1995* Vol. 1 (AIP Conf. Proc., No. 370, Eds S C Schmidt, W C Tao) (Woodbury, NY: American Institute of Physics, 1996) p. 121
16. Trunin R F *Usp. Fiz. Nauk* **164** 1215 (1994) [*Phys. Usp.* **37** 1123 (1994)]
17. Zhugin Yu N et al. *Fiz. Zemli* (6) 46 (1999) [*Izv., Phys. Solid Earth* **35** 478 (1999)]
18. Petrovtsev A V et al. "Equation of state and phase diagram quartz", in *Shock Compression of Condensed Matter — 2005* (AIP Conf. Proc., CP 845, Ed. M D Furnish) (Melville, NY: American Institute of Physics, 2006) (in press)
19. Simonenko V A "Vozmozhnosti izucheniya uravnenii sostoyaniya plotnykh veshchestv v oblasti proyavleniya obolochechnykh effektov" ("Prospects for equation of states studies on dense materials in the strong shell effect region") *Voprosy At. Nauki Tekh. Ser. Teor. Prikl. Fiz.* ((1)) 3 (1984)
20. Sin'ko G V "Raschety termodinamicheskikh funktsii prostykh veshchestv na osnove uravneniya sostoyaniya samosoglasovannogo polya" ("Calculation of thermodynamic functions for simple substances using a self-consistent field equation of state"), in *Chislennye Metody Mekhaniki Sploshnoi Sredy* (Numerical Methods in Mechanics of Continua) Vol. 10, Issue 3 (Novosibirsk: VTs ITPM SO AN SSSR, 1979) p. 124
21. Andriyash A V, Simonenko V A "Otsenka vliyaniya obolochechnykh effektov na termodinamicheskie svoistva prostykh veshchestv" ("Estimating shell effects on the thermodynamic properties of simple substances") *Voprosy At. Nauki Tekh. Ser. Teor. Prikl. Fiz.* (2(2)) 52 (1984)
22. Avrorin E N et al. *Zh. Eksp. Teor. Fiz.* **93** 613 (1987) [*Sov. Phys. JETP* **66** 347 (1980)]
23. Vodolaga B K, Simonenko V A "Udarnye issledovaniya i matematicheskoe modelirovanie" ("Shock studies and mathematical modeling"), in *Fiziko-Khimicheskie Svoistva Veshchestva* (Physical and Kinematic Properties of Matter) (Editors-in-Chief A A Samarskii, N N Kalitkin) (Moscow: Nauka, 1989)
24. Simonenko V A et al. *Zh. Eksp. Teor. Fiz.* **88** 1452 (1985) [*Sov. Phys. JETP* **61** 869 (1985)]
25. Ragan C E (III), Silbert M G, Diven B C *J. Appl. Phys.* **48** 2860 (1977)
26. Simonenko V A et al. "Defending the Earth against impacts from large comets and asteroids", in *Hazards Due to Comets and Asteroids* (Ed. T Gehrels) (Tucson: Univ. of Arizona Press, 1994) p. 929
27. Simonenko V A "O korrektirovke dvizheniya asteroidov s pomoshch'yu yadernykh vzryvov" ("Using nuclear explosions to divert asteroids") *Rossiiskii Kosmos* (3) (2002); Simonenko V A, Gadzhieva V V, Elsukov V P "Ob opasnosti stolknoveniya kosmicheskikh tel s Zemlei i ee predotvrashchenii" ("The danger and prevention of Earth's encounters with space bodies"), in *Zababakhinskie Nauchnye Chteniya: Mezhdunar. Konf., 8 – 12 Sent. 2003, Snezhinsk, Chelyab. obl., Russia. Tezisy* (Zababakhin Scientific Talks: Intern. Conf. 8 – 12 Sep. 2003, Snezhinsk, Chelyabinsk region, Russia. Theses) (Snezhinsk: Izd. RFYaTs — VNIITF, 2003) p. 214
28. Simonenko V A "Neitronnye zvezdy i yadernye vzryvy" ("Neutron stars and nuclear explosions"), in *Voprosy Sovremennoi Tekhnicheskoi Fiziki: K 70-letiyu so Dnya Rozhdeniya Akad. E.N. Avrorina. Izbrannye Trudy RFYaTs — VNIITF* (Problems in Modern Engineering Physics: on the Occasion of the 70th Birthday of Academician E.N. Avrorin. Selected Works of RFYaTs — VNIITF) (Ed. G N Rykovanov, Compiled by G N Rykovanov et al.) (Snezhinsk: Izd. RFYaTs — VNIITF, 2002) p. 391
29. Simonenko V A et al. "Termoyadernye vspyshki neitronnykh zvezd: usloviya vozniknoveniya i rezhimy goreniya" ("Thermonuclear bursts of neutron stars: conditions for and regimes of combustion"), in *Zababakhinskie Nauchnye Chteniya: Mezhdunar. Konf. 8 – 12 Sent. 2003, Snezhinsk, Chelyab. obl., Russia. Tezisy* (Zababakhin Scientific Talks: Intern. Conf. 8 – 12 Sep. 2003, Snezhinsk, Chelyabinsk region, Russia. Theses) (Snezhinsk: Izd. RFYaTs — VNIITF, 2003) p. 5
30. Simonenko V A, Shishkin N I "Termoyadernye vspyshki neitronnykh zvezd: initsiirovanie vtorichnoi volny goreniya v antipode oblasti pervichnogo initsiirovaniya" ("Thermonuclear bursts of neutron stars: of the secondary burning wave in the antipode area

of primary ignition''), in *Zababakhinskie Nauchnye Chteniya: Mezhdunar. Konf. 8–12 Sent. 2003, Snezhinsk, Chelyab. obl., Russia. Tezisy* (Zababakhin Scientific Talks: Intern. Conf. 8–12 Sep. 2003, Snezhinsk, Chelyabinsk region, Russia. Theses) (Snezhinsk: Izd. RFYaTs — VNIITF, 2003) p. 106

PACS numbers: 75.30.Sg, **75.80.+q**, 81.30.Kf
DOI: 10.1070/PU2006v049n08ABEH006081

Magnetic shape-memory alloys: phase transitions and functional properties

V D Buchelnikov, A N Vasiliev, V V Koledov, S V Taskaev, V V Khovaylo, V G Shavrov

1. Introduction

The discovery of the effect of giant deformations due to a magnetically induced rearrangement of martensite twins in Heusler alloys Ni_2MnGa [1] attracted significant attention to shape-memory alloys. As a result of intense research in this field, magnetically induced strains as large as 10%, which can be controlled by a magnetic field of about 1 T, have been realized in Ni-Mn-Ga single crystals, and a number of new families of ferromagnets with a shape-memory effect have been revealed [2].

In this report, we review the art and science of theoretical and experimental investigations of phase transitions in ferromagnetic Heusler alloys with the shape-memory effect and of related giant changes in entropy and strain under the effect of an applied magnetic field. Attention is mainly paid to new results concerning the investigations of Ni-Mn-Ga alloys. In particular, we analyze the results of investigations of the specific features of the phase diagram of these alloys and their physical properties in the nanocrystalline state.

2. Magnetic and structural phase transitions

2.1 Phenomenological theories

To describe phase transitions in Ni-Mn-Ga alloys, we first consider the Landau functional [3–8]

$$
\begin{aligned}
F = {} & -Ae_1 + \frac{1}{2}\,A_0 e_1^2 + \frac{1}{2}\,a_1(e_2^2+e_3^2) + De_1(e_2^2+e_3^2) \\
& + \frac{1}{3}\,be_3(e_3^2-3e_2^2) + \frac{1}{4}\,c(e_2^2+e_3^2)^2 + \frac{1}{2}\,A_1|\psi|^2 + \frac{1}{4}\,A_2|\psi|^4 \\
& + \frac{1}{6}\,C_0|\psi|^6 + \frac{1}{6}\,C_1\left[\psi^6 + (\psi^*)^6\right] \\
& + \left(\frac{1}{\sqrt{3}}\,D_1e_1 + \frac{2}{\sqrt{6}}\,D_2e_3 + D_3e_4\right)|\psi|^2 + \frac{1}{2}\,\alpha_1\mathbf{m}^2 + \frac{1}{4}\,\delta_1\mathbf{m}^4 \\
& + K(m_x^2m_y^2 + m_y^2m_z^2 + m_z^2m_x^2) + \frac{1}{\sqrt{3}}\,B_1e_1\mathbf{m}^2 \\
& + B_2\left[\frac{1}{\sqrt{2}}\,e_2(m_x^2-m_y^2) + \frac{1}{\sqrt{6}}\,e_3(3m_z^2-\mathbf{m}^2)\right] \\
& + B_3(e_4m_xm_y + e_5m_ym_z + e_6m_zm_x) \\
& + \left[N_1\mathbf{m}^2 + N_2\left(m_z^2 - \frac{1}{3}\,\mathbf{m}^2\right) + N_3m_xm_y\right]|\psi|^2 + Pe_1\,, \quad (1)
\end{aligned}
$$

where e_i are the linear combinations of the strain tensor components: $e_1 = (e_{xx}+e_{yy}+e_{zz})/\sqrt{3}$, $e_2 = (e_{xx}-e_{yy})/\sqrt{2}$, $e_3 = (2e_{zz}-e_{yy}-e_{xx})/\sqrt{6}$, $e_4 = e_{xy}$, $e_5 = e_{yz}$, $e_6 = e_{zx}$; ψ is the order parameter that describes the modulation of the crystal lattice and is related to the displacement vector $\mathbf{u}$ along the $[\bar{1}10]$ axis as $\mathbf{u}(\mathbf{r}) = |\psi|\mathbf{p}\sin(\mathbf{kr}+\varphi)$, where $\psi = |\psi|\exp(i\varphi)$, $\mathbf{k} = (1/3)[110]$, and $\mathbf{p}$ is the polarization vector; A is a coefficient proportional to the thermal expansion coefficient; $A_0 = (c_{11}+2c_{12})/\sqrt{3}$ is the bulk elasticity modulus; a_1, b, D, and c_1 are linear combinations of elasticity moduli of the second, third, and fourth orders,

$$
a_1 = c_{11} - c_{12}\,, \qquad b = \frac{c_{111} - 3c_{112} + 2c_{123}}{6\sqrt{6}}\,,
$$

$$
D = \frac{c_{111} - c_{123}}{2\sqrt{3}}\,, \qquad c = \frac{c_{1111} + 6c_{1112} - 3c_{1122} - 8c_{1123}}{48}\,;
$$

$\mathbf{m} = \mathbf{M}/M_0$ is the unit magnetization vector; M_0 is the saturation magnetization; B_1 is the constant of volume (exchange) magnetostriction; B_2 and B_3 are the constants of anisotropic (relativistic) magnetostriction; K is the first constant of cubic anisotropy; α_1 and δ_1 are the exchange constants; A_1, A_2, C_0, and C_1 are the coefficients of the expansion of the functional into a series in powers of the modulation order parameter ψ; D_i are the coupling coefficients of the deformation and modulation order parameters; N_i are the coupling constants of the modulation order parameter to the magnetization; and P is the hydrostatic pressure.

The equilibrium states of a cubic ferromagnet can be determined from thermodynamic potential (1) using the standard minimization procedure. The solution of this problem, which can be found both analytically and numerically, has been obtained in several works (see [2] and the references therein).

We note that in $Ni_{2+x}Mn_{1-x}Ga$ alloys, the sign of the first cubic anisotropy constant K depends on the composition [9, 10]. Therefore, the cases where $K > 0$ and $K < 0$ must be considered within a theoretical description of phase transitions (see Refs [66, 67, 91, 200–210] and [211–215] in [2] for $K < 0$ and $K > 0$, respectively).

Investigations of the effect of magnetostriction and modulation of the crystal lattice on the phase transition in Ni-Mn-Ga alloys show that, with the modulation order parameter taken into account, the martensitic transformation is accompanied by either premartensitic or intermartensitic phase transitions [7, 11].

Taking the magnetoelastic interaction into account leads to the appearance of a domain of the existence of combined magnetic and structural (magnetostructural) phase transitions in the phase diagram of $Ni_{2+x}Mn_{1-x}Ga$ alloys [12, 13]. Estimates show that the magnetostructural phase transition in the temperature–composition ($T-x$) phase diagram is realized in a very narrow range of x. Recent experimental studies of the $T-x$ phase diagram of Ni-Mn-Ga alloys in a wider composition range [14] showed that the magnetostructural transition is realized in a rather wide composition interval from $x = 0.18$ to $x = 0.27$ (Fig. 1). In this concentration range, the alloys undergo a transition from a cubic paramagnetic phase into a tetragonal ferromagnetic phase. In this transformation, we can therefore neglect the magnetostriction related to anisotropy and consider only the volume magnetostriction, which is usually large just in the region of a magnetic phase transition. The phase diagram